Dynamic model of a municipal wastewater stabilization pond in the arctic

Recio-Garrido, Didac; Kleiner, Yehuda; Colombo, Andrew; Tartakovsky, Boris

Publisher's version / Version de l'éditeur:
https://doi.org/10.1016/j.watres.2018.07.052
Water Research, 144, pp. 444-453, 2018-07-20

Dynamic Model of a Municipal Wastewater Stabilization Pond in the Arctic

Didac Recio-Garrido[1], Yehuda Kleiner[2], Andrew Colombo[2], and Boris Tartakovsky[1*]

National Research Council of Canada
[1]6100 Royalmount Ave, Montreal, QC, Canada H4P 2R2
[2]12000 Montreal Rd, Ottawa, ON, Canada K1A 0R6

Waste stabilisation ponds (WSPs) are the method of choice for sewage treatment in most arctic communities because they can operate in extreme climate conditions, they require a relatively modest investment, they are passive and therefore easy and inexpensive to operate and maintain. However, most arctic WSPs are currently limited in their ability to remove carbonaceous biochemical oxygen demand (CBOD), total suspended solids (TSS) and ammonia-nitrogen. An arctic WSP differs from a 'southern' WSP in the way it is operated and in the conditions under which it operates. Consequently, the existing WSP models cannot be used to gain better understanding of the arctic lagoon performance. This work describes an Arctic-specific WSP model. The model accounts for both aerobic and anaerobic degradation pathways of organic materials and considers the periodic nature of WSP operation as well as the partial or complete freeze of the water in the WSP during winter. A multi-layer approach was taken in the model development, which significantly simplified and expedited model solution, enabling efficient model calibration to available field data.

Keywords: Arctic, facultative lagoon, WSP, dynamic model

* corresponding author
phone: 514-496-2664
e-mail: Boris.Tartakovsky@cnrc-nrc.gc.ca

1. INTRODUCTION

Waste stabilisation ponds (WSPs, also called "sewage lagoons" or "facultative lagoons") are used for secondary treatment of municipal sewage by many small communities around the globe because they require a relatively modest investment, they are easy and inexpensive to operate and maintain by locally available personnel. WSPs are the method of choice for sewage treatment in most Canadian arctic communities because they can operate in extreme climate conditions. However, most arctic WSPs are currently limited in their ability to remove carbonaceous biochemical oxygen demand (CBOD), total suspended solids (TSS) and ammonia-nitrogen.

There are some fundamental differences between WSPs operated in the Arctic and those operated elsewhere. Whereas in non-Arctic settings the lagoon is always full (constant water volume) and is operated as a flow-through system, the extreme sub-zero temperatures in the Arctic winter do not allow for any outflow of effluent, as this would freeze instantly. Moreover, as the sewage in the arctic lagoon is ice-capped during most of the year, a low organic removal rate can be expected during this cold period. As a result, the typical Arctic WSP has a volume designed to accommodate an entire year of sewage production with the sewage flowing into the WSP during the year. The WSP is typically emptied (decanted) in late summer to early fall (in some locations WSPs are decanted slowly during the entire summer). After decanting, the WSP is ready to receive the next year's sewage production. These conditions make all existing WSP models unsuitable for simulating Arctic WSPs.

Despite the simplicity of WSP design and the practical experience gained from its use for several decades all around the world, a complete understanding of all the physical, chemical and biological processes involved is still an ongoing area of research [*Sah et al.*, 2012]. Some kinetic

and stoichiometric parameters for the biochemical processes can be assumed from well-established models used in other domains, e.g. ADM1 [*Batstone et al.*, 2002] and ASM3 [*Henze et al.*, 2000]. Current WSP models concentrate on describing only some of the complex interactions occurring in such systems. Many of the existing models focus on hydrodynamics for a better WSP geometry design in 1D, 2D or 3D [*Aldana et al.*, 2005; *Martínez et al.*, 2014; *Sah et al.*, 2011; *Salter et al.*, 2000; *Sweeney et al.*, 2003], whilst others assume simplified hydraulic conditions (completely mixed or plug flow) and focus on the biochemical processes for a better understanding of the biodegradation processes and effluent quality [*Beran and Kargi*, 2005; *Dochain et al.*, 2003; *Houweling et al.*, 2005; *Peng et al.*, 2007]. Other models still, focus primarily on describing the sedimentation mechanisms of the particulates [*Jupsin and Vasel*, 2007; *Toprak*, 1994] or the daily [*Kayombo et al.*, 2000] or seasonal [*Banks et al.*, 2003; *Chaturvedi et al.*, 2014] oxygen dynamics. Temperature profiles have also been the object of study and modeling in WSP operated in moderate climates [*Gu and Stefan*, 1995; *Sweeney et al.*, 2005]. More recently, the coupling of hydrodynamic equations with biochemical processes produced a complex 3D model [*Sah et al.*, 2011] that provides a detailed component distribution in the lagoon. However, such 3D models are difficult to calibrate, given existing scarce experimental data, often lacking measurements at different lagoon depths and locations.

The literature reflects scant information with regard to calibration and validation of models with full-scale WSP data [*Sah et al.*, 2012]. In the Arctic, this dearth of WSP field data is even greater due to extreme winter conditions and remoteness of WSP locations [*Ragush et al.*, 2015]. The formation of a thick ice cover in Arctic lagoons for 6 to 8 months of the year (depending on location) increases modeling complexity as it affects all physical and biological mechanisms of COD removal. This study attempts to close the gap by developing a dynamic

model of a WSP, which accounts for periodic nature of lagoon operation in the Arctic and considers the impact of ice cover on WSP performance.

2. MODEL FORMULATION

2.1 Modeling approach

The proposed model uses a multi-layer approach to describe the existence of several distinct zones in a facultative lagoon. The multi-layer approach to modeling was successfully applied in the past to various biological systems with significant oxygen, carbon source, or biomass gradients [*Rauch et al.*, 1999; *Tartakovsky and Guiot*, 1997]. Accordingly, the model assumes the existence of three distinct layers at any given time, each assumed to be completely mixed. In the relatively warm period in the summer, the top layer is assumed to be aerobic liquid, the middle layer anaerobic liquid, and the bottom layer is sludge, assumed to always be under anaerobic conditions. The depth of the aerobic layer is expected to be restricted to 20 – 50 cm due to limited oxygen penetration (no forced aeration) and fast oxygen consumption by aerobic bacteria [*Hunik et al.*, 1994; *Stephenson et al.*, 1999; *Tartakovsky et al.*, 2006].

In the cold period the WSP is assumed to be completely ice-capped, which means that there is no oxygen flow from the air into the liquid (the depletion of oxygen in the liquid due to icing is nearly instantaneous). Consequently, there is no aerobic layer during the cold season. The anaerobic layer of liquid can become partially or completely frozen, depending on ambient temperature. The sludge layer is assumed to remain in a liquid state due to its depth as well as due to exothermic microbial activities such as hydrolysis of solids and anaerobic biodegradation of soluble organics, which result in heat production and help to prevent the sludge layer from freezing.

Figure 1 shows a schematic diagram of the layers considered during the warm and cold periods. During the warm season the depth (or thickness) of the aerobic layer (z^{AE}) is considered to be constant, while the depth of the anaerobic (z^{AN}) and the sludge (z^{SL}) layers increases as a result of the daily addition of raw wastewater.

2.2 Icecap modeling

A separate model was developed to estimate the thickness of ice as a function of the ambient temperature profiles (degree days). This model was developed based on work by Ashton et al [*Ashton*, 1986; 1989] with modifications to account for the heat flux from the relatively warm sewage inflow to the ice layer and for the insulating properties of snow cover. A detailed description of the icecap model is provided in Supplementary Information (Appendix A). The direct coupling of the icecap model to the multi-layer lagoon model would have resulted in more complex computations and a slower combined model with a marginal improvement in accuracy. Instead, the icecap model is used to estimate the time at which the icecap begins to form, the time at which it reaches maximum thickness, and the time at which it completely melts. The maximum icecap thickness is also estimated. These estimated values are subsequently used in the lagoon model under the simplifying assumption of constant rate of freeze (ice growth) and constant rate of ice thaw.

2.3 Biodegradation modeling

In formulating the biodegradation, several simplifying assumptions were made towards reducing model integration time and facilitating model calibration. Although ADM1 and ASM3 models consider multiple microbial populations, in the absence of Arctic-specific data on the distribution of microbial populations, the proposed model only aerobic heterotrophic ($X_{B,H}$) and anaerobic ($X_{B,AN}$) microorganisms. These populations are assumed to be present in all layers.

Also, only readily biodegradable soluble (S_s) and particulate (X_s) organic materials are considered in the material balances, i.e., the current version of the model does not include nitrogen and phosphorus balances.

The aerobic and anaerobic liquid layers are assumed to have a saturation (maximal attainable) concentration (X_{max}) of suspended solids. At the end of each day of model integration, the solids in excess of this saturation concentration are assumed to settle directly into the sludge layer. Another simplifying assumption is that removal (or settling) of solids from the aerobic and anaerobic layers to the sludge layer is instantaneous. Also, all dissolved components are assumed to be uniformly distributed between the layers (instant mixing assumption). The instantaneous settling and mixing assumptions can be justified by the fact that the lagoon performance is simulated over a period of one year. Therefore the settling and mixing processes occurring at a scale of several hours or even days may be considered instantaneous without any significant loss of accuracy.

Material balances and kinetic equations describing the hydrolysis of particulate organic materials and the growth of $X_{B,H}$ and $X_{B,AN}$ microbial populations on soluble organic materials were adapted from ASM3 [*Henze et al.*, 2000]. In particular, multiplicative Monod kinetic equations are used to describe aerobic and anaerobic (anoxic) growth of heterotrophic biomass, which is dependent on readily available dissolved substrate (S_s) and dissolved oxygen (S_O) concentrations, i.e.

$$\mu_H = \mu_{max,H}\left(\frac{S_S}{K_{S,H}+S_S}\right)\left(\frac{S_O}{K_{O,H}+S_O}\right)X_{B,H}+\mu_{max,H}\left(\frac{S_S}{K_{S,H}+S_S^i}\right)\left(\frac{K_{O,I}}{K_{O,I}+S_O}\right)X_{B,H}, \qquad (1)$$

where μ_H is the specific growth rate of the aerobic heterotrophic microorganisms, $\mu_{max,H}$ is the maximum specific growth rate of the heterotrophs, $K_{S,H}$ and $K_{O,H}$ are the half saturation constants, and $K_{O,I}$ is the inhibition constant.

The specific growth rate of anaerobic microorganisms (μ_{AN}) is described as

$$\mu_{AN} = \mu_{max,AN}\left(\frac{S_S}{K_{S,AN}+S_S}\right)\left(\frac{K_{O,I}}{K_{O,I}+S_O}\right)\left(\frac{K_{AN,I}}{K_{AN,I}+X_{B,AN}}\right)X_{B,AN}\ , \quad (2)$$

where $\mu_{max,AN}$ is the maximum specific growth rate of the anaerobes, $K_{S,AN}$ is the half-saturation constant of anaerobic microorganisms and $K_{AN,I}$ is the self-inhibition constant.

The rate of hydrolysis of particulate materials plays an important role in determining the outcome of wastewater treatment, as it often represents the slowest biodegradation step. The following expression, adapted from ASM3 model, is used to describe the specific hydrolysis rate (r_h) in the proposed model, where both aerobic and anaerobic populations contribute to the hydrolysis:

$$r_h = k_{h,H}\left(\frac{X_S^i/\left(X_{B,H}^i+X_{B,AN}^i\right)}{K_{X,H}+X_S^i/(X_{B,H}^i+X_{B,AN}^i)}\right)(X_{B,H}^i + \eta X_{B,AN}^i), \quad (3)$$

where $k_{h,H}$ is the maximum hydrolysis rate, $k_{X,H}$ and $k_{B,H}$ are the half saturation constants of hydrolysis and η is the fraction of anaerobes($X_{B,AN}$) contributing to hydrolysis.

The rates of aerobic and anaerobic degradation of soluble organic materials are assumed to be proportional to the growth rates of the corresponding microbial populations. A detailed description of these equations and the material balances of the model are provided in Supplementary Information (Appendix B).

2.4 Numerical methods

At each moment in time the performance of the WSP is described by the COD concentration in the lagoon (total - COD_t, soluble - COD_s and particulate - COD_p) calculated as

$$COD_p = \frac{1}{V_t}\sum_i\left(X_S^i + X_I^i\right)V^i \quad (4)$$

$$COD_s = \frac{1}{V_t}\sum_i \left(S_S^i + S_I^i\right)V^i \quad (5)$$

$$COD_t = COD_s + COD_p \quad (6)$$

where V_t is the combined volume of all layers (volume of the lagoon content), i is the layer index, $i = AE, IC, AN, SL$ corresponding to the aerobic, ice, anaerobic, and sludge layers.

First-order differential equations, corresponding to the model material balances, are numerically solved using *ODE45* function of Matlab R2010 (Mathworks, Natick, MA, USA). Model parameters are estimated using Matlab's unconstrained optimization function *fminsearch*, to minimize the root mean squared error (RMSE) between estimated and observed values of total, soluble and particulate COD concentrations:

$$RMSE_{Tot} = \sqrt{\sum_k \left(\frac{1}{N_k}\sum_{j=1}^{N_k}\left(y_{k,j}^{obs} - y_{k,j}^{mod}\right)^2\right)}\,. \quad (7)$$

Here, N_k is the total number of measurements; y^{obs} represents experimentally measured (or observed) values; y^{mod} represents the corresponding model output (estimated) values; k is the index corresponding to COD components, $\mathrm{k} = \{COD_t, COD_s, COD_p\}$.

As will be described later, the sensitivity of model results to parameter values was used in the calibration/validation process. The relative sensitivity s_k of each model parameter θ with respect to each output variable y_k was computed as:

$$s_k = \frac{\partial y_k}{\partial \theta_j} \cdot \frac{\theta_j}{y_k} \quad (8)$$

where $k = \{COD_t, COD_s, COD_p\}$ and j is the parameter's index.

3. MODEL CALIBRATION AND VALIDATION

The proposed model was calibrated and validated using data collected at three arctic lagoons situated in the hamlets of Pond Inlet, Gjoa Haven, and Kugaruuk (Nunavut, Canada).

182 The three are engineered lagoons, with surface areas (when full) of about 40,000, 20,000, 13,000
183 m^2, and average depths (when full) of about 1.6, 3 and 3 m, respectively.

184 Available measurements at these lagoons included characterization of raw sewage and
185 samples withdrawn from the lagoons (typically near the discharge point) during one year. Only
186 two to three sampling campaigns per year were carried out at each location, typically in early or
187 mid-summer as well as late-summer or early fall, towards decanting. Information provided
188 through these campaigns in include total and soluble COD and/or BOD concentration, and total
189 suspended solid (TSS) concentration. If total COD concentration values were unavailable, they
190 were estimated using BOD_5 measurements by assuming a COD to BOD_5 ratio of 2 (i.e., 1 mg L^{-1}
191 of BOD_5 is equivalent to 2 mg L^{-1} of COD). Pond Inlet lagoon characterization results were
192 taken from [*Ragush et al.*, 2015], while measurements at Gjoa Haven, and Kugaruuk were
193 provided by Environment Canada (unpublished data corresponding to lagoon characterization
194 from September 2009 to September 2010). Also, daily temperatures, precipitation (rain and
195 snow) and depth of snow on the ground at each location were obtained from the publicly
196 available Environment Canada website for the corresponding years and used for icecap
197 formation/melting dates and thickness computations.
198

199 **3.1 Icecap formation**

200 The icecap formation and decay model described in Appendix A was used to estimate the
201 beginning and end of ice formation as well as the icecap thickness. Figure 2 shows the resulting
202 ice thickness profiles calculated for the Pond Inlet, Gjoa Haven, and Kugaruuk lagoons in
203 Nunavut, Canada, based on the temperature profiles from September 2009 to September 2010. In
204 the fall of 2009 icecap started forming around September 15th to September 20th (relatively soon

after decant) in all three locations. Consequently, September 15th was considered as t = 0 (see Figure 2) for the model calibration calculations. The calculations of ice thickness were carried out for 350 days. Water discharge was assumed to take place between days 350 – 365 (not shown in Figure 2) and effective average snow cover thickness was assumed to be 50% of the "snow on the ground" values provided by Environment Canada data.

As can be seen from Figure 2, at all three locations a near constant ice formation rate is estimated, resulting in a linear increase of ice thickness up to about day 200. Subsequently, a constant ice thickness is estimated between days 200-270, followed by a period of relatively fast thaw that culminates with ice-free surface at about day 295. It should be noted that only 50% of the accumulated snow on the ground (as recorded by Environment-Canada) was effectively considered for heat-flux calculations, as a portion of the snow was assumed to have been blown away due to winds.

As mentioned earlier, the ice-formation model was not directly coupled with the lagoon model. Rather, these simulation results were used to determine ice formation parameters (start of ice formation and thaw as well as constant ice formation and thaw rates), which were used as inputs for the multi-layer lagoon model.

3.2 Biodegradation kinetics

Initially, model parameters related to aerobic heterotrophic activity were taken from ASM3 [*Henze et al.*, 2000], while degradation rates under anaerobic conditions were assumed from [*Lettinga et al.*, 2001]. Also, initial value of the oxygen transfer coefficient (k_L) was adapted from the work of Chaturvedi et al. [*Chaturvedi et al.*, 2014], assuming wind speeds between 1 and 8 m s^{-1} and an average water temperature of 10 ºC. Table 1 provides the values of all model

parameters and Tables 2 and 3 describe influent wastewater composition and initial conditions used for model integration.

Considering the rather large number of model parameters and the limited number of available measurements (only 2-3 sets of COD and TSS measurements were available for each lagoon, with no biomass measurements at all), it was deemed best to identify a small subset of model parameters with the largest influence on model outputs and subsequently calibrate the model using only this limited subset, while all other parameters are kept constant at values obtained from the literature. The most influential parameters were identified through a sensitivity analysis, using Eq. 8. Table 4 summarizes results of this sensitivity analysis. Based on these results, a subset of three parameters was selected for estimation, namely the maximum specific growth rate of anaerobic microorganisms ($\mu_{max,AN}$), the rate of solid organic matter hydrolysis (k_h), and the oxygen transfer coefficient (k_L).

Parameter estimation (model calibration) was performed using data of two lagoons, Pond Inlet and Gjoa Haven, whereby values of parameters $\mu_{max,an}$, k_h, and k_L that minimized RMSE (Eq. 7) were identified (all other parameters were held constant). Figure 3 provides the resulting profiles of total, soluble, and particulate CODs for the Pond Inlet and Gjoa Haven lagoons with the calibrated parameters. Table 5 summarizes the estimated values of these parameters. The model was subsequently validated by applying the estimated parameter values to the Kugaruuk lagoon. Figure 4 illustrates a comparison between estimated and observed values of COD and TSS measurements in the Kugaaruk lagoon.

It can be seen that in all cases the model predicted a COD accumulation during winter months followed by a relatively fast COD degradation during the ice-free period. While the predicted trends qualitatively agreed with the observed values, the RMSE value for Kugaruuk

validation was higher (as expected) than for the lagoons used for parameter estimation (Table 5). It was nonetheless deemed that the model showed a reasonable capability to correctly predict the measured trends in total and dissolved COD concentrations.

As mentioned earlier, the small number of measured data available for calibration presented a significant challenge to the confidence with which the results could be evaluated. Consequently, an additional calibration method was undertaken whereby the estimation procedure was repeated for each lagoon individually. In this case however, the oxygen transfer coefficient was kept at the estimated value of 6.4 m d^{-1} , while $\mu_{max,an}$ and $k_{h,H}$ values were re-estimated for each lagoon. As shown in Table 5, this approach resulted in smaller RMSE values and also demonstrated the differences between the lagoons in terms of $\mu_{max,an}$ and $k_{h,H}$ values. Since parameter sensitivity analysis showed high impact of these parameters on the model outputs, the differences between the lagoons are likely represented by the differences between lagoon-specific values.

4. DISCUSSION

While the dearth of calibration data limits the confidence in the accuracy of the results, some important, and not altogether expected, trends on the performance of facultative sewage lagoons in the Arctic can be discerned from the model outputs. For example, a clear trend emerges, whereby soluble COD concentration increases consistently during winter months (Figures 3, 4). This can be explained by the fact that during winter, particulate COD settles and continuously undergoes hydrolysis in the sludge layer of the lagoon, albeit at a low rate, while at the same time a relatively slow anaerobic degradation acts to reduce soluble COD concentration. When the icecap melts away, fast reduction in soluble COD concentration can be observed, as

aerobic activity initiates and increases in the top layer. The aerobic growth of suspended heterotrophic biomass is accompanied by biomass settling, since the suspended biomass concentration in the aerobic layer is limited by the maximum attainable density (X_{max}). The aerobic biomass in the sludge layer contributes to hydrolysis of solids according to Eq. (3). Notably, the hydrolysis rate is not limited by the absence of oxygen in the sludge. As a result, the overall rate of hydrolysis accelerates during summer.

Another important observation can be made that although the degradation of organic materials under anaerobic conditions is slow (compared to aerobic degradation), the anaerobic activity provides a significant contribution to the overall COD removal in the lagoon due to the fact that this activity takes place throughout the year and also due to the high sludge density. This can be further demonstrated by comparing different scenarios of COD degradation in the shallow Pond Inlet lagoon (Figure 5A) and the deep Kugaruuk lagoon (Figure 5B). In one scenario the COD degradation is simulated with the anaerobic rate of COD degradation set to zero (only aerobes), while in the other scenario the aerobic degradation rate is set to zero (only anaerobes). It is clear that the absence of anaerobic biodegradation throughout the winter results in COD accumulation in both lagoons. If zero anaerobic activity is assumed, the rate of aerobic degradation required to achieve observed COD concentrations at the end of summer would have to be increased to an unrealistically high value of approximately 10 d^{-1}, which is not likely given that water temperature in the lagoons does not typically exceed 10-12^{o}C during the summer. Clearly, only a combination of both aerobic and anaerobic degradation activities results in the COD profiles matching the field measurements.

Interestingly, the model predicts different COD profiles during winter for each lagoon. Pond Inlet lagoon is relatively shallow (about 1.6 m average depth when full), in which the ice

297 thickness can reach a maximum of about 1.4 m (Figure 2). This results in an expected gradual
298 increase of total and soluble COD concentrations throughout the winter due to the absence of
299 biological activity in the ice layer. Although, anaerobic degradation continues in the sludge layer,
300 it is not sufficient to considerably reduce soluble CODs (Figure 3). This prediction agrees well
301 with the high COD value measured at the beginning of summer, right after the complete melting
302 of the ice cover. This accumulation of CODs is followed by a relatively fast COD reduction in
303 the summer. It can be seen that even in the shallow Pond Inlet lagoon anaerobic degradation
304 contributes to the overall COD removal as the comparison of different scenarios shown in Figure
305 5A indicates.

306 The predicted COD profiles in the much deeper Gjoa Haven, and Kugaruuk lagoons followed
307 a somewhat different pattern. In these lagoons a fast increase in COD concentrations is predicted
308 during the first 50-60 days, followed by slow COD concentration decrease throughout the winter,
309 due to anaerobic activity in the unfrozen anaerobic and sludge layers under the ice. The rate of
310 COD degradation is predicted to accelerate during the summer (Figures 3 and 4) due to aerobic
311 activity. It is noted (again) that only COD trends in the summer months can be confirmed by
312 observed data. Profiles of particulate CODs in all lagoons were similar with a somewhat higher
313 concentration during summer. Fast growth of aerobic bacteria in the upper oxygenated layer
314 during summer months results is accompanied by biomass settling, which contributes to
315 particulate CODs as well as to sludge accumulation, although it increases the rate of hydrolysis
316 according to model equation (3). Notably, solids hydrolysis does not require dissolved oxygen
317 and therefore proceeds in the sludge layer, where the biomass concentration is the highest.

318 A detailed look at the model outputs and the parameter estimation results suggests that
319 the difference in COD profiles can be explained by the differences in lagoon depths. The shallow

Pond Inlet lagoon is frozen during 260 days of the year (most of this period frozen through, except the sludge layer), which significantly limits anaerobic activity during winter months. During the summer months a high degradation rate is achieved due to higher ratio of aerobic to anaerobic activity. In Pond Inlet, an aerobic layer thickness of 40 cm corresponds to approximately 25% of this lagoon depth, while in two other lagoons the aerobic layer comprises less than 15% of the total lagoon depth. Consequently, aerobic degradation provides a relatively higher contribution to COD removal at the Pond Inlet lagoon compared to two other, deeper lagoons (Figure 5).

Gradual degradation of COD throughout winter in the Gjoa Haven and Kugaruuk lagoons is attributed to the existence of a liquid anaerobic layer throughout the winter months (Figures 3, 4), which supports anaerobic activity. As a result, a moderate COD concentration decrease is predicted, despite the presence of the icecap.

The importance of considering anaerobic microbial activity in northern lagoons appears to be an immediate conclusion, with important implications for future lagoon design. It can be surmised that some combination of deep and shallow lagoons is likely to provide the best results in terms of degradation of organics in the sewage. In fact, there is some evidence that multi-cell lagoons in the Arctic are functioning well. It appears that a deep first lagoon is likely to provide substantial anaerobic degradation in winter, while a shallow and wide second lagoon will provide substantial aerobic degradation in summer.

Another important consideration in evaluating Arctic lagoon performance could be related to the contribution of algae blooms to COD removal. While the current version of the model does not consider algae growth, it appears to be indirectly accounted for by the oxygen transfer coefficient (k_L). During long summer days algae are expected to supply oxygen to the

343 top (aerobic) layer of the lagoon. Indeed, parameter estimation yielded a k_L value of 6.4, which is
344 somewhat higher than a range of values suggested in literature (0.9 – 6.0 m d^{-1}), as indicated in
345 Table 1. In addition to increased oxygen supply, both phototrophic and heterotrophic growth of
346 algae are likely to contribute to solids accumulation, especially after the end of summer, when
347 temperatures become lower and days become shorter, before the formation of icecap. Future
348 version of the Arctic lagoon model needs to be extended to account for this phenomenon as well
349 as for nitrogen and phosphorus removal at low temperatures.
350

351 **5. CONCLUSION**

352 This study describes a mathematical model capable of simulating the biodegradation of
353 wastewater in arctic WSPs. The model accounts for several unique features of Arctic lagoons,
354 including the periodic nature of lagoon operation and the existence of icecap for most of the
355 lagoon operation cycle. The proposed model is calibrated and validated using limited observed
356 data, obtained at three arctic lagoons. Acceptable agreement between the predicted and measured
357 COD and TSS concentration profiles was obtained. Analysis of predicted COD concentration
358 profiles suggests significant anaerobic biodegradation of organic materials throughout winter
359 months. The model can be used for analyzing and improving Arctic lagoon design.
360

361 **Acknowledgement**

362 The authors wish to acknowledge Environment and Climate Change Canada (ECCC) and in
363 particular Ms. Shirley Anne Smyth, who provided unpublished data that were invaluable for the
364 initial calibration of the model. Also Mr. Babesh Roy of the Government of Nunavut, who
365 facilitated data sharing on the Pond Inlet lagoon.

366 **Notations**

A	Lagoon's surface, m^2
a	Specific interfacial area, m^{-1}
BOD	Biological oxygen demand, mg L^{-1}
b_{AN}	Decay rate of $X_{B,AN}$*, d^{-1}
b_H	Decay rate of $X_{B,H}$*, d^{-1}
COD	Chemical oxygen demand, mg L^{-1}
CSTR	Continuous stirred tank reactor
f_P	Fraction of X_B yielding X_S, %
h	Lagoon's depth, m
$K_{AN,I}$	Self-inhibition coefficient for $X_{B,AN}$, mg L^{-1}
K_L	Oxygen mass transfer coefficient**, m d^{-1}
$K_{O,H}$	Half-saturation coefficient of S_O for $X_{B,H}$, mg L^{-1}
$K_{O,I}$	Inhibition coefficient of S_O for $X_{B,H}$, mg L^{-1}
$K_{S,AN}$	Half-saturation coefficient of S_S for $X_{B,AN}$, mg L^{-1}
$K_{S,H}$	Half-saturation coefficient of S_S for $X_{B,H}$, mg L^{-1}
$K_{X,H}$	Half-saturation coefficient of X_S for $X_{B,H}$, mg L^{-1}
k_h	Maximum specific hydrolysis rate*, d^{-1}
MSE	Mean squared error
q_{in}	Input flow rate, L d^{-1}
$q_{tr}^{i\to j}$	Transfer flow rate from layer i to layer j, L d^{-1}
S_O	Concentration of soluble oxygen, mg L^{-1}
$S_{O,max}$	Maximum value for S_O, mg L^{-1}
S_I	Concentration of soluble inert materials, mg L^{-1}
S_s	Concentration of biodegradable soluble substrate, mg L^{-1}
t_{ini}^{ICE}	Start of ice formation, d
t_{end}^{ICE}	End of ice thaw, d
V	Lagoon's volume, L
WSP	Wastewater stabilization pond

$X_{B,AN}$ Concentration of heterotrophic bacteria, mg L^{-1}

$X_{B,H}$ Concentration of anaerobic bacteria, mg L^{-1}

X_I Concentration of particulate inerts, mg L^{-1}

$X_{max}^{AE,AN}$ Solids saturation density in liquid, mg L^{-1}

X_{max}^{S} Solids saturation density in sludge, mg L^{-1}

X_{max}^{IC} Solids saturation density in ice, mg L^{-1}

X_S Concentration of biodegradable particulate substrate, mg L^{-1}

$Y_{S,H}$ Yield factor of S_S for $X_{B,H}$ mg/mg

$Y_{S,AN}$ Yield factor of S_S for $X_{B,AN}$mg/mg

$Y_{O,H}$ Yield factor of S_O for $X_{B,H}$, mg/mg

z layer height, m

z_{max}^{AE} Maximum thickness aerobic layer, m

z_{max}^{IC} Maximum thickness of ice layer, m

α Solids settling, %

Δt^{IC} Period of ice formation/thaw, d

η_h Correction factor for hydrolysis by $X_{B,AN}$*

η_g Correction factor anoxic growth $X_{B,H}$

$\mu_{max,H}$ Maximum specific growth rate of $X_{B,H}$*, d^{-1}

$\mu_{max,AN}$ Maximum specific growth rate of $X_{B,AN}$*, d^{-1}

Indices

AE Aerobic layer

AN Anaerobic layer

end Final

exp Experimental values

H Heterotrophic microbial population

h Related to hydrolysis

I Inert

IC Ice layer

i or j Any of the layers in the model

in	Influent
ini	Initial
max	Maximum
O	Oxygen, S_O, mg L^{-1}
SL	Sludge layer or related to the soluble substrate
sim	Simulated values
tr	Transfer between layers

367

368

369

370 **REFERENCES**

371 Aldana, G. J., B. J. Lloyd, K. Guganesharajah, and N. Bracho (2005), The development and
372 calibration of a physical model to assist in optimising the hydraulic performance and design of
373 maturation ponds, *Water Sci. Technol.*, *51*(12), 173-181.

374 Ashton, G. D. (1983), *Predicting Lake Ice Decay*, Cold regions research and engineering lab
375 Hanover NH.

376 Ashton, G. D. (1986), *River and lake ice engineering*, Water Resources Publication.

377 Ashton, G. D. (1989), Thin ice growth, *Water Resour. Res.*, *25*(3), 564-566.

378 Banks, C. J., G. B. Koloskov, A. C. Lock, and S. Heaven (2003), A computer simulation of the
379 oxygen balance in a cold climate winter storage WSP during the critical spring warm-up period,
380 *Water Sci. Technol.*, *48*(2), 189-196.

381 Batstone, D. J., J. Keller, I. Angelidaki, S. V. Kalyuzhnyi, S. G. Pavlostathis, A. Rozzi, W. T. M.
382 Sanders, H. Siegrist, and V. A. Vavilin (2002), The IWA anaerobic digestion model no 1
383 (ADM1), *Water Sci. Technol.*, *45*(10), 65-73.

384 Beran, B., and F. Kargi (2005), A dynamic mathematical model for wastewater stabilization
385 ponds, *Ecol. Model.*, *181*(1), 39-57.

386 Borja, R., E. González, F. Raposo, F. Millán, and A. Martín (2002), Kinetic analysis of the
387 psychrophilic anaerobic digestion of wastewater derived from the production of proteins from
388 extracted sunflower flour, *J. Agric. Food Chem.*, *50*(16), 4628-4633.

389 Chaturvedi, M. K. M., S. D. Langote, D. Kumar, and S. R. Asolekar (2014), Significance and
390 estimation of oxygen mass transfer coefficient in simulated waste stabilization pond, *Ecol. Eng.*,
391 *73*, 331-334.

392 Chen, Y. R., and A. G. Hashimoto (1978), Kinetics of methane fermentation, paper presented at
393 Biotechnol. Bioeng. Symp.
394 Dochain, D., S. Gregoire, A. Pauss, and M. Schaegger (2003), Dynamical modelling of a waste
395 stabilisation pond, *Bioprocess. Biosyst. Eng.*, *26*(1), 19-26.
396 Gu, R., and H. G. Stefan (1995), Stratification dynamics in wastewater stabilization ponds,
397 *Water Res.*, *29*(8), 1909-1923.
398 Henze, M., W. Gujer, T. Mino, and M. C. M. van Loosdrecht (2000), *Activated sludge models*
399 *ASM1, ASM2, ASM2d and ASM3*, IWA publishing.
400 Houweling, C. D., L. Kharoune, A. Escalas, and Y. Comeau (2005), Modeling ammonia removal
401 in aerated facultative lagoons, *Water Sci. Technol.*, *51*(12), 139-142.
402 Hunik, J. H., C. G. Bos, M. P. Hoogen, C. D. DeGooijer, and J. Tramper (1994), Co-
403 immobilized Nitrosomonas europea and Nitrobacter agilis cells: validation of a dynamic model
404 for simultaneous substrate conversion and growth in k-carrageenan gel beads, *Biotechnol.*
405 *Bioeng.*, *43*, 1153-1163.
406 Jupsin, H., and J. L. Vasel (2007), Modelisation of the contribution of sediments in the treatment
407 process case of aerated lagoons, *Water Sci. Technol.*, *55*(11), 21-27.
408 Kayombo, S., T. S. A. Mbwette, A. W. Mayo, J. H. Y. Katima, and S. E. Jorgensen (2000),
409 Modelling diurnal variation of dissolved oxygen in waste stabilization ponds, *Ecol. Model.*,
410 *127*(1), 21-31.
411 Langergraber, G., D. P. L. Rousseau, J. García, and J. Mena (2009), CWM1: a general model to
412 describe biokinetic processes in subsurface flow constructed wetlands, *Water Sci. Technol.*,
413 *59*(9), 1687-1697.

414 Lettinga, G., S. Rebac, and G. Zeeman (2001), Challenge of psychrophilic anaerobic wastewater
415 treatment, *Trends Biotechnol.*, *19*(9), 363-370.
416 Martínez, F. C., A. T. Cansino, M. A. A. García, V. Kalashnikov, and R. L. Rojas (2014),
417 Mathematical analysis for the optimization of a design in a facultative pond: indicator organism
418 and organic matter, *Math. Probl. Eng.*, *2014*.
419 Peng, J. F., B. Z. Wang, Y. H. Song, and P. Yuan (2007), Modeling N transformation and
420 removal in a duckweed pond: model development and calibration, *Ecol. Model.*, *206*(1), 147-
421 152.
422 Perry, R., and D. Green (1984), *Perry's Chemical Engineers' Handbook, McGraw-HiII*, Inc.
423 NewYork.
424 Ragush, C. M., J. J. Schmidt, W. H. Krkosek, G. A. Gagnon, L. Truelstrup-Hansen, and R. C.
425 Jamieson (2015), Performance of municipal waste stabilization ponds in the Canadian Arctic
426 *Ecological Eng.*, *83*, 413-421.
427 Rauch, W., H. Vanhooken, and P. A. Vanrolleghem (1999), A simplified mixed-culture biofilm
428 model, *Wat. Res.*, *33*, 2148-2162.
429 Sah, L., D. P. L. Rousseau, and C. M. Hooijmans (2012), Numerical modelling of waste
430 stabilization ponds: where do we stand?, *Water Air Soil Pollut.*, *223*(6), 3155-3171.
431 Sah, L., D. P. L. Rousseau, C. M. Hooijmans, and P. N. L. Lens (2011), 3D model for a
432 secondary facultative pond, *Ecol. Model.*, *222*(9), 1592-1603.
433 Salter, H. E., C. T. Ta, S. K. Ouki, and S. C. Williams (2000), Three-dimensional computational
434 fluid dynamic modelling of a facultative lagoon, *Water Sci. Technol.*, *42*(10-11), 335-342.
435 Stephenson, R. J., A. Patoine, and S. R. Guiot (1999), Effects of oxygenation and upflow liquid
436 velocity on a coupled anaerobic/aerobic reactor system, *Wat. Res.*, *33*, 2855-2863.

437 Sweeney, D. G., J. B. Nixon, N. J. Cromar, and H. J. Fallowfield (2005), Profiling and modelling
438 of thermal changes in a large waste stabilisation pond, *Water Sci. Technol.*, *51*(12), 163-172.
439 Sweeney, D. G., N. J. Cromar, J. B. Nixon, C. T. Ta, and H. J. Fallowfield (2003), The spatial
440 significance of water quality indicators in waste stabilization ponds-limitations of residence time
441 distribution analysis in predicting treatment efficiency, *Water Sci. Technol.*, *48*(2), 211-218.
442 Tartakovsky, B., and S. R. Guiot (1997), Modeling and analysis of layered stationary anaerobic
443 granular biofilms, *Biotechnol. Bioeng.*, *54*, 122-130.
444 Tartakovsky, B., M. F. Manuel, and S. R. Guiot (2006), Degradation of trichloroethylene in a
445 coupled anaerobic-aerobic bioreactor : modeling and experiment, *Biochemical Engineering*
446 *Journal*, *26*(1), 72-81.
447 Toprak, H. (1994), Empirical modelling of sedimentation which occurs in anaerobic waste
448 stabilization ponds using a lab-scale semi-continuous reactor, *Environ. Technol.*, *15*(2), 125-134.
449 van der Berg, L. (1977), Effect of temperature on growth and activity of a methanogenic culture
450 utilising acetate, *Can. J. Microbiol.*, *23*(7), 898-902.
451
452
453
454
455
456
457

458 **Table 1.** Values of the lagoon model parameters.

Parameter	Value	Notes	Source	Range
$\mu_{max,H}$	3[1]	Assumed	[*Henze et al.*, 2000]	0.6 – 13.2
$\mu_{max,AN}$	0.09 – 0.12[1]	Calibrated	[*Batstone et al.*, 2002] [*van der Berg*, 1977] [*Chen and Hashimoto*, 1978] [*Borja et al.*, 2002]	0.05 – 8
b_H	0.05[1]	Assumed	[*Henze et al.*, 2000]	0.05-1.6
b_{AN}	0.02[1]	Assumed	[*Batstone et al.*, 2002]	-
$K_{S,H}$	20	Assumed	[*Henze et al.*, 2000]	5-225
$K_{S,AN}$	28	Assumed	[*Batstone et al.*, 2002] [*Langergraber et al.*, 2009] [*Borja et al.*, 2002]	28 - 150
$K_{O,H}$	0.2	Assumed	[*Henze et al.*, 2000] [*Banks et al.*, 2003]	0.01 – 0.2
$K_{X,H}$	0.01	Assumed	[*Henze et al.*, 2000]	0.01 – 0.03
k_h	0.10 - 0.22`[1]	Calibrated	[*Henze et al.*, 2000]	1-3
η_h	0.1[1]	Assumed	[*Henze et al.*, 2000] [*Langergraber et al.*, 2009]	0.1-0.4
$K_{O,I}$	0.2	Assumed	[*Henze et al.*, 2000]	0.01 – 0.2
$K_{AN,I}$	200	Assumed	-	-
$S_{O,max}$	12	Assumed	[*Perry and Green*, 1984] [*Sah et al.*, 2011]	7-15
K_L	6.4[2]	Calibrated	[*Chaturvedi et al.*, 2014]	0.86 – 6.04
a	0.32 - 0.6	Measured	-	-
η_g	0	Assumed	[*Henze et al.*, 2000]	0.6 –.0
$Y_{S,H}$	1.58	Assumed	[*Henze et al.*, 2000]	1.33 – 2.63
$Y_{S,AN}$	1.3	Assumed	[*Batstone et al.*, 2002]	-
$Y_{O,H}$	1.72	Assumed	[*Henze et al.*, 2000]	-
f_P	0.08	Assumed	[*Henze et al.*, 2000]	0.08
A	11,093-36,686	Measured	this work	-
h	1.65-3.13	Measured	this work	-
t_{ini}^{IC}	10	Calculated	this work	-
t_{end}^{IC}	295	Calculated	this work	-
Δt^{IC}	30	Calculated	this work	-
z_{max}^{IC}	1.2 - 1.5	Calculated	this work	-
α	90	Assumed	this work	-
$X_{max}^{AE,AN}$	32.0-70.3	Measured	this work	-
X_{max}^{SL}	8,000	Assumed	this work	-
X_{max}^{IC}	infinite	Assumed	this work	-
z_{max}^{AE}	0.4	Assumed	this work	-

459 [1] Set to zero in the ice layer

460 [2] Only considered for the aerobic layer

461 **Table 2.** Influent wastewater composition.

WW component	Notation	Dimension	Value	Notes
Heterotrophic biomass	$X_{B,Hin}$	mg L^{-1}	5	Assumed
Anaerobic biomass	$X_{B,ANin}$	mg L^{-1}	5	Assumed
Soluble biodegradable substrate	$S_{s,in}$	mg L^{-1}	1010[1]; 789[2]; 775[3]	Measured
Particulate biodegradable substrate	$X_{S,in}$	mg L^{-1}	460[1]; 391[2]; 366[3]	Measured
Dissolved oxygen	$S_{O,in}$	mg L^{-1}	0	Assumed
Particulate inert substrate	$X_{I,in}$	mg L^{-1}	0	Assumed
Soluble inert substrate	$S_{I,in}$	mg L^{-1}	0	Assumed
Flow rate	q_{in}	m^3 d^{-1}	138.1[1]; 128.2[2]; 85.1[3]	Measured

462 [1]Pond Inlet lagoon, [2]Gjoa Haven lagoon, and [3]Kugaruuk lagoon

463

464 **Table 3**. Initial conditions used for lagoon model integration.

Parameter	Dimension	Layer				Notes
		Aerobic	Anaerobic	Sludge	Ice	
$X_{B,H}$	mg L^{-1}	10	0	0	0	Assumed
$X_{B,AN}$	mg L^{-1}	0	10	100	0	Assumed
S_s	mg L^{-1}	260[1]; 200[2,3]	260[1]; 200[2,3]	260[1]; 200[2,3]	0	Measured[1] Assumed[2,3]
X_S	mg L^{-1}	64[1]; 50[2,3]	64[1]; 50[2,3]	X_{max}^{SL}	0	Measured[1] Assumed[2,3]
S_O	mg L^{-1}	3.5	0	0	0	Measured
X_I	mg L^{-1}	0	0	0	0	Assumed
S_I	mg L^{-1}	0	0	0	0	Assumed
z	m	z_{max}^{AE}	0	0.02	0	Assumed

465
466 [1]Pond Inlet lagoon, [2]Gjoa Haven lagoon, and [3]Kugaruuk lagoon
467
468

Table 4. Parameter sensitivity values with respect to COD_t, COD_p, *and* COD_s variations.

Parameter	s_{COD_t}	s_{COD_p}	s_{COD_s}
$\mu_{max,H}$	-12.6	-6.8	-15.5
$\mu_{max,AN}$	710.4	-256.9	968.8
b_H	48.8	5.5	59.9
b_{AN}	57.8	0.9	69.8
$K_{S,H}$	-2.6	13.9	-5.4
$K_{O,H}$	0.8	0.2	1.0
$K_{X,H}$	0.1	-0.1	0.2
k_h	-5484.9	285.4	-6760.8
η_h	85.1	14.5	124.0
$K_{O,I}$	-0.4	-0.1	-0.5
K_L	-430.5	-997.9	-387.3
z_{max}^{AE}	1.0	-3.8	2.3

473

474 **Table 5**. Model calibration and validation results. Notations: PI – Pond Inlet lagoon, GH - Gjoa

475 Haven, and KU – Kugaruuk.

476

Lagoon	K_L	k_h	$\mu_{max,AN}$	**RMSE**	**Notes**
PI and GH	6.40	0.043	0.07	197	calibration
KU	6.40	0.043	0.07	195	validation
PI	6.40	0.100	0.11	63	re-calibration
GH	6.40	0.220	0.09	69	re-calibration
KU	6.40	0.22	0.12	102	re-calibration

477

478

479

480

481

482

483

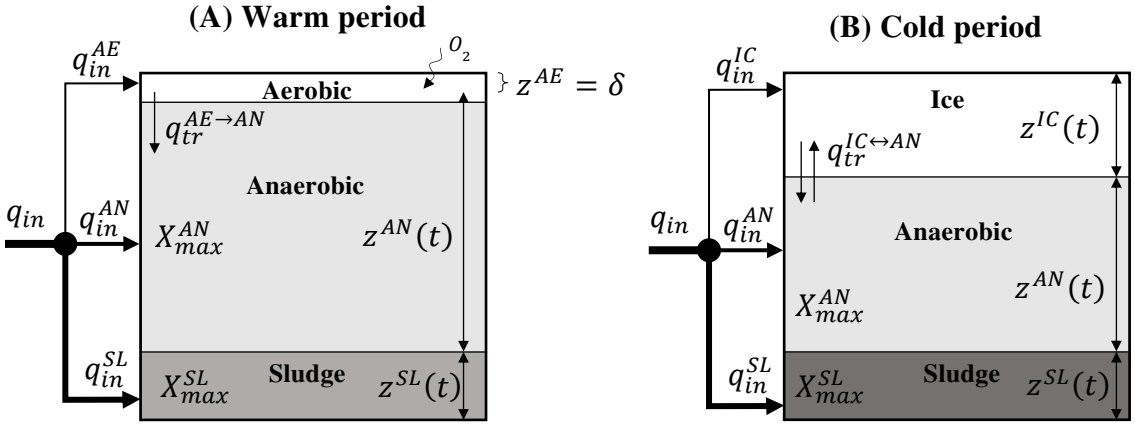

Figure 1. Schematic diagram of the layers considered in the model during (A) warm and (B) cold periods.

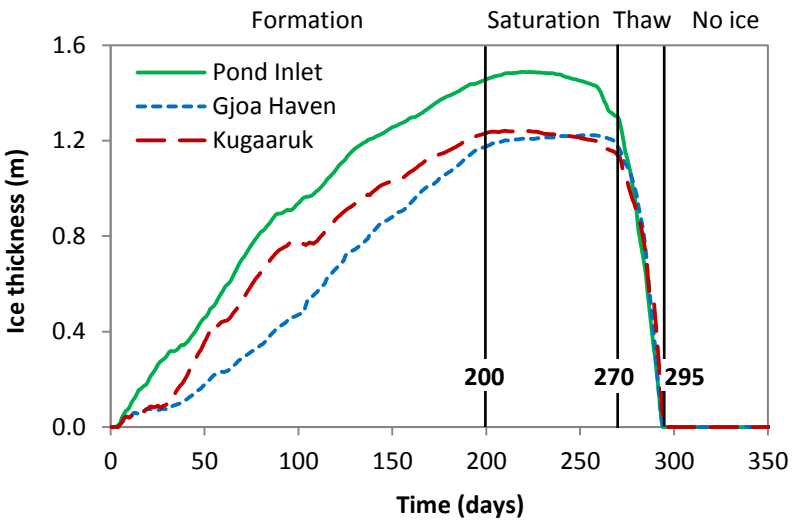

Figure 2. Icecap profile simulated using temperature data collected in 2010. Ice thickness values are presented from September 15th 2009 (day 0) until August 31st ,2010 (day 350).

517

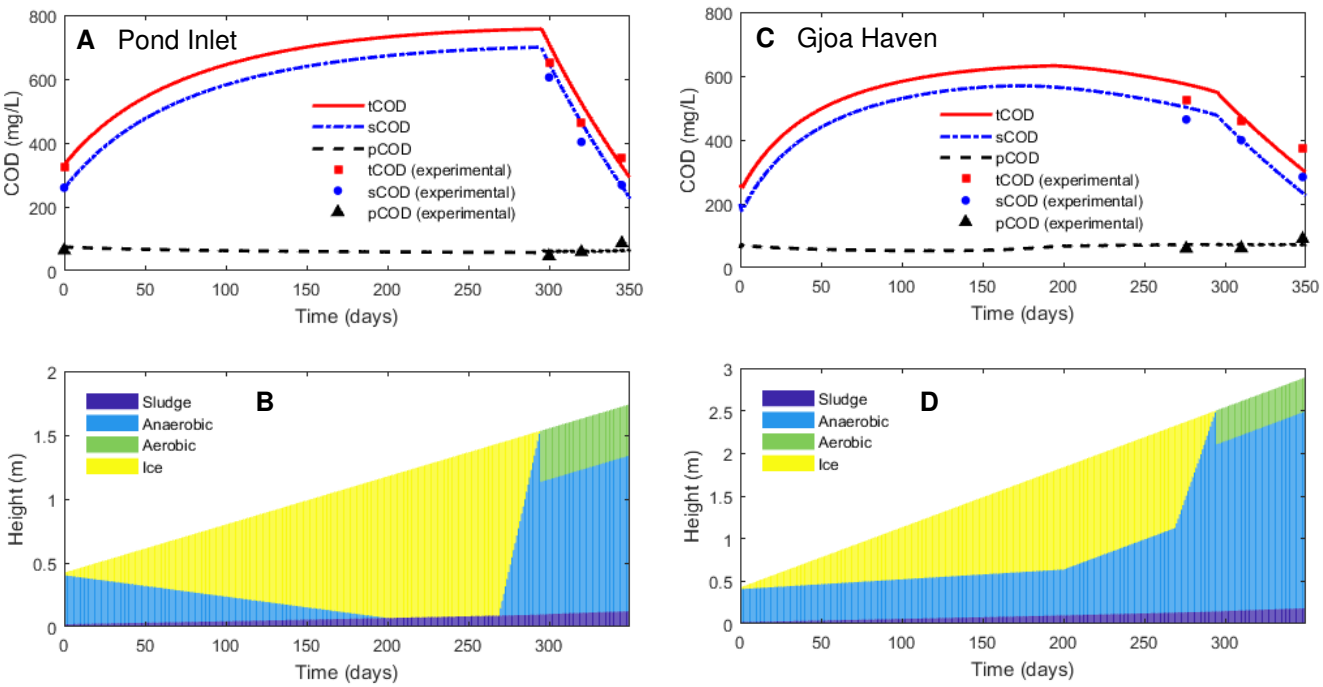

528

529

530

531

532

533

534

535

536 **Figure 3.** Model calibration results showing a comparison of model outputs with experimental

537 data and predicted layer thickness for (A, B) Pond Inlet and (C, D) Gjoa Haven lagoons.

538

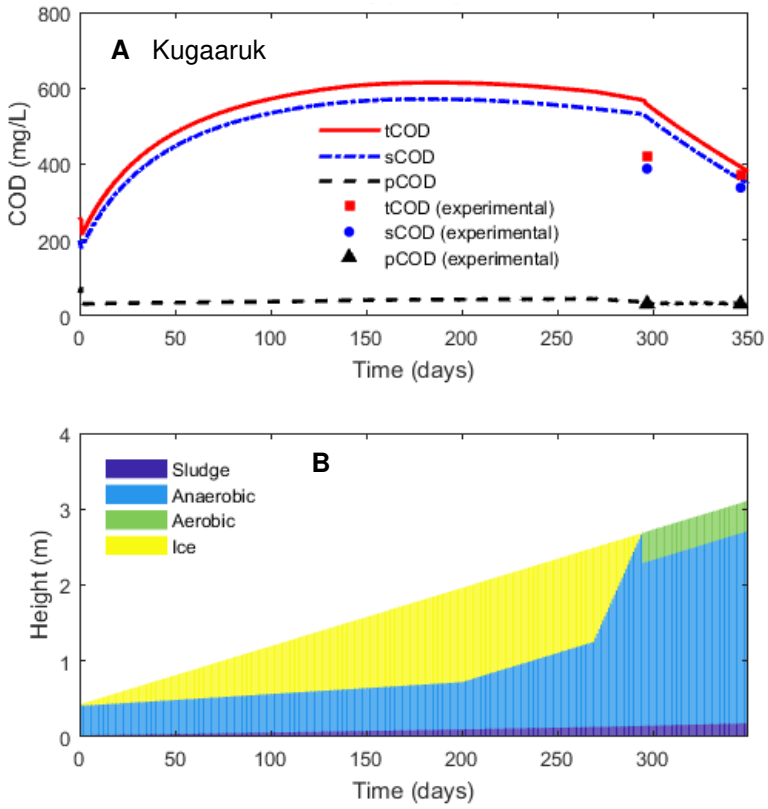

Figure 4. Model validation results showing a comparison of model outputs with experimental data (A) and predicted layer thickness (B) for Kugaruuk lagoon.

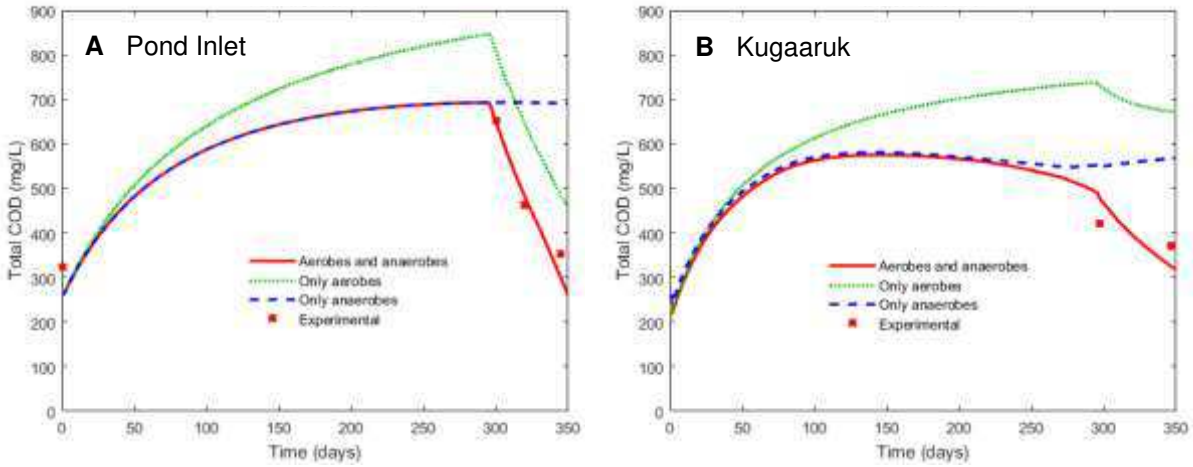

Figure 5. A comparison of COD concentration profiles calculated with and without contribution of aerobic and anaerobic degradation for the Pond Inlet (A) and Kugaaruk (B) lagoons.

584 **SUPPLEMENTARY INFORMATION**

585 **APPENDIX A. Modelling icecap formation and decay**

586 The following equation was used to describe ice formation. This equation is based on
587 work by Ashton [*Ashton*, 1986; 1989] with modifications to account for the heat flux from the
588 relatively warm sewage inflow to the ice layer and for the insulating properties of snow cover:

$$\Delta h = \left(\frac{\Delta t}{\rho L}\right)\left[\frac{T_m - T_a}{\left(\frac{h_i}{k_i} + \frac{h_s}{k_s} + \frac{1}{H_a}\right)} - H_{wi}(T_w - T_m)\right] \quad \text{(A1)}$$

589 where

590 Δh = incremental growth of ice layer thickness [m] over time-step Δt

591 k_i = thermal conductivity of ice [W m^{-1} $^oC^{-1}$] (taken as 2.3 (corresponding to temp. of
592 about -10 ^oC) for this research)

593 k_s = thermal conductivity of snow [W m^{-1} $^oC^{-1}$] (taken as 0.4 for this research)

594 T_m = temperature at the ice water interface (assumed 0^oC)

595 T_w = temperature of the water under the ice

596 T_a = temperature of air above the ice [^oC]

597 H_a = thermal resistance (or heat transfer coefficient) between the uppermost surface and
598 the air above it (i.e., when $h_s = 0$ then $H_a = H_{ia}$; and when $h_s > 0$ then $H_a = H_{as}$)

599 H_{ia} = bulk heat transfer coefficient between the top surface temperature of the ice and the
600 air temperature above the ice (taken as 25 [W m^{-2} $^oC^{-1}$] for this research

601 H_{sa} = bulk heat transfer coefficient between the top surface temperature of snow and the
602 air temperature above the snow (taken as 15 [W m^{-2} $^oC^{-1}$] for this research)

603 H_{wi} = bulk heat transfer coefficient between the water and the ice (taken as 2.19 [W m^{-2}
604 $^oC^{-1}$] for this research

605 ρ = ice density [kg/m^{-3}] (taken as 919 (corresponding to temp. of about -10 ^{o}C) for this
606 research)
607 L = heat of fusion [J/kg^{-1}] (taken as 3.3355•10^{5} for this research)
608 h_i = thickness of the ice cover at time-step Δt
609 h_s = thickness of the snow cover at time-step Δt

610 When Δt is taken as one day (or 86,400 seconds) the ice layer thickness becomes a
611 function of freezing degree-days.

612 The following equation was used to model the decay of ice over a sewage lagoon. This
613 equation is also based on work by Ashton [*Ashton*, 1983] with modifications to account for the
614 heat flux from the relatively warm sewage inflow to the ice layer:

$$\Delta h = \left(\frac{\Delta t}{\rho L}\right)[-H_{ia}(T_m - T_a) - H_{wi}(T_w - T_m)] \quad \text{(A2)}$$

615 Here too, when Δt is taken as one day the ice layer thickness becomes a function of
616 melting degree-days. In the absence of real field data, the water temperature T_w is assumed to
617 have a sinusoidal form over the year with an amplitude of A_{Tw} and a period of 365 days. The
618 average temperature in day d is therefore estimated as:

$$T_{W_d} = T_{W_{min}} + 0.5A_{T_W}\left[1 + cos\frac{2\pi d}{365}\right] \quad (d = 1, 2, \ldots 365) \quad \text{(A3)}$$

619 where d =1 is the day at which decanting ends. Minimum water temperature $T_{W_{min}}$ was assumed
620 to be 3^{o}C. The amplitude can be expected to be in the range of 4 to 12 degrees.

621

622

APPENDIX B. Biodegradation model

The following material balance equations are used to describe sewage biodegradation. The balances are composed for each layer I, where $i, j = AE, AN, SL, IC$ and $j \neq i$.

1. Heterotrophic biomass ($X^i_{B,H}$)

$$\frac{dX^i_{B,H}}{dt} = \underbrace{\mu_{max,H}\left(\frac{S^i_S}{K_{S,H}+S^i_S}\right)\left(\frac{S^i_O}{K_{O,H}+S^i_O}\right)X^i_{B,H}}_{\text{Aerobic growth of heterotrophic biomass}} + \underbrace{\eta_g\mu_{max,H}\left(\frac{S^i_S}{K_{S,H}+S^i_S}\right)\left(\frac{K_{O,I}}{K_{O,I}+S^i_O}\right)X^i_{B,H}}_{\text{Anoxic growth of heterotrophic biomass}}$$

$$- \underbrace{b_H X^i_{B,H}}_{\substack{\text{Decay of}\\ \text{heterotrophic biomass}}} + \underbrace{\frac{q^i_{in}}{V^i}\left(X_{B,Hin}-X^i_{B,H}\right)}_{\text{Flow in}} + \underbrace{\frac{q^{j\to i}_{tr}}{V^i}\left(X^j_{B,H}-X^i_{B,H}\right)}_{\text{Transport term}}$$

2. Anaerobic biomass ($X^i_{B,AN}$)

$$\frac{dX^i_{B,AN}}{dt} = \underbrace{\mu_{max,AN}\left(\frac{S^i_S}{K_{S,AN}+S^i_S}\right)\left(\frac{K_{O,I}}{K_{O,I}+S^i_O}\right)\left(\frac{K_{AN,I}}{K_{AN,I}+X^i_{B,AN}}\right)X^i_{B,AN}}_{\text{Growth of anaerobic biomas}} - \underbrace{b_{AN}X^i_{B,AN}}_{\substack{\text{Decay of}\\ \text{anaerobic biomass}}}$$

$$+ \underbrace{\frac{q^i_{in}}{V^i}\left(X_{B,AN,in}-X^i_{B,AN}\right)}_{\text{Flow in}} + \underbrace{\frac{q^{j\to i}_{tr}}{V^i}\left(X^j_{B,AN}-X^i_{B,AN}\right)}_{\text{Transport term}}$$

628 **3. Readily biodegradable soluble substrate (S_s^i)**

$$\frac{dS_s^i}{dt} = \underbrace{-Y_{S,H}\mu_{max,H}\left(\frac{S_S^i}{K_{S,H}+S_S^i}\right)\left(\frac{S_O^i}{K_{O,H}+S_O^i}\right)X_{B,H}^i}_{\text{Aerobic growth of heterotrophic biomass}} \underbrace{-\eta_g Y_{S,H}\mu_{max,H}\left(\frac{S_S^i}{K_{S,H}+S_S^i}\right)\left(\frac{K_{O,I}}{K_{O,I}+S_O^i}\right)X_{B,H}^i}_{\text{Anoxic growth of heterotrophic biomass}}$$

$$\underbrace{-Y_{S,AN}\mu_{max,AN}\left(\frac{S_S^i}{K_{S,AN}+S_S^i}\right)\left(\frac{K_{O,I}}{K_{O,I}+S_O^i}\right)\left(\frac{K_{AN,I}}{K_{AN,I}+X_{B,AN}^i}\right)X_{B,AN}^i}_{\text{Growth of anaerobic biomas}}$$

$$\underbrace{+k_{h,H}\left(\frac{X_S^i/\left(X_{B,H}^i+X_{B,AN}^i\right)}{K_{X,H}+X_S^i/\left(X_{B,H}^i+X_{B,AN}^i\right)}\right)\left(X_{B,H}^i+\eta X_{B,AN}^i\right)}_{\text{Hydrolysis of entrapped particulate organics}} \underbrace{+\frac{q_{in}^i}{V^i}\left(S_{s,in}-S_s^i\right)}_{\text{Flow in}}$$

$$\underbrace{+\frac{q_{tr}^{j\to i}}{V^i}\left(S_s^j-S_s^i\right)}_{\text{Transport term}}$$

629 **4. Slowly biodegradable particulate substrate (X_S^i)**

$$\frac{dX_S^i}{dt} = \underbrace{(1-f_P)b_H X_{B,H}^i}_{\substack{\text{Decay of}\\ \text{heterotrophic biomass}}} + \underbrace{(1-f_P)b_{AN}X_{B,AN}^i}_{\substack{\text{Decay of}\\ \text{anaerobic biomass}}} + \underbrace{\frac{q_{in}^i}{V^i}\left(X_{S,in}-X_S^i\right)+\underbrace{\frac{q_{tr}^{j\to i}}{V^i}\left(X_s^j-X_s^i\right)}_{\text{Transfer flow}}}_{\text{Flow in}}$$

$$\underbrace{-k_{h,H}\left(\frac{X_S^i/\left(X_{B,H}^i+X_{B,AN}^i\right)}{K_{X,H}+X_S^i/\left(X_{B,H}^i+X_{B,AN}^i\right)}\right)\left(X_{B,H}^i+\eta X_{B,AN}^i\right)}_{\text{Hydrolysis of entrapped particulate organics}}$$

630 **5. Soluble oxygen (S_O^i)**

$$\frac{dS_O^i}{dt} = \underbrace{-Y_{O,H}\mu_{max,H}\left(\frac{S_S^i}{K_{S,H}+S_S^i}\right)\left(\frac{S_O^i}{K_{O,H}+S_O^i}\right)X_{B,H}^i}_{\text{Consumption by aerobic growth of heterotrophic biomass}} + \underbrace{K_L a\left(S_{O,max}-S_O^i\right)}_{\text{Transfer term}} + \underbrace{\frac{q_{in}^i}{V^i}\left(S_{O,in}-S_O^i\right)}_{\text{Flow in}}$$

$$\underbrace{+\frac{q_{tr}^{j\to i}}{V^i}\left(S_O^j-S_O^i\right)}_{\text{Transfer flow}}$$

631 **6. Inert particulate (X_I^i)**

$$\frac{dX_I^i}{dt} = \underbrace{f_P b_H X_{B,H}^i}_{\text{Decay of heterotrophic biomass}} + \underbrace{f_P b_{AN} X_{B,AN}^i}_{\text{Decay of anaerobic biomass}} + \underbrace{\frac{q_{in}^i}{V^i}\left(X_{I,in} - X_I^i\right)}_{\text{Flow in}} + \underbrace{\frac{q_{tr}^{j\to i}}{V^i}\left(X_I^j - X_I^i\right)}_{\text{Transfer flow}}$$

632 **7. Soluble inert organic (S_I^i)**

$$\frac{dS_I^i}{dt} = \underbrace{\frac{q_{in}^i}{V^i}\left(S_{I,in} - S_I^i\right)}_{\text{Flow in}} + \underbrace{\frac{q_{tr}^{j\to i}}{V^i}\left(S_I^j - S_I^i\right)}_{\text{Transfer flow in}}$$

633 **8. Height (depth) of the layer (z^i)**

$$\frac{dz^i}{dt} = \underbrace{\frac{q_{in}^i}{A}}_{\text{Flow in}} \pm \underbrace{\frac{q_{tr}^{j\to i}}{A}}_{\text{Transfer flow}}$$

634

635 **9. Recalculation of initial conditions (instant settling of solids)**

636 Figure B1 explains the simplified approach for describing the settling of solids produced
637 by microbial growth. This calculation is used after each day of integration. Solids redistribution
638 is not considered in the ice layer.

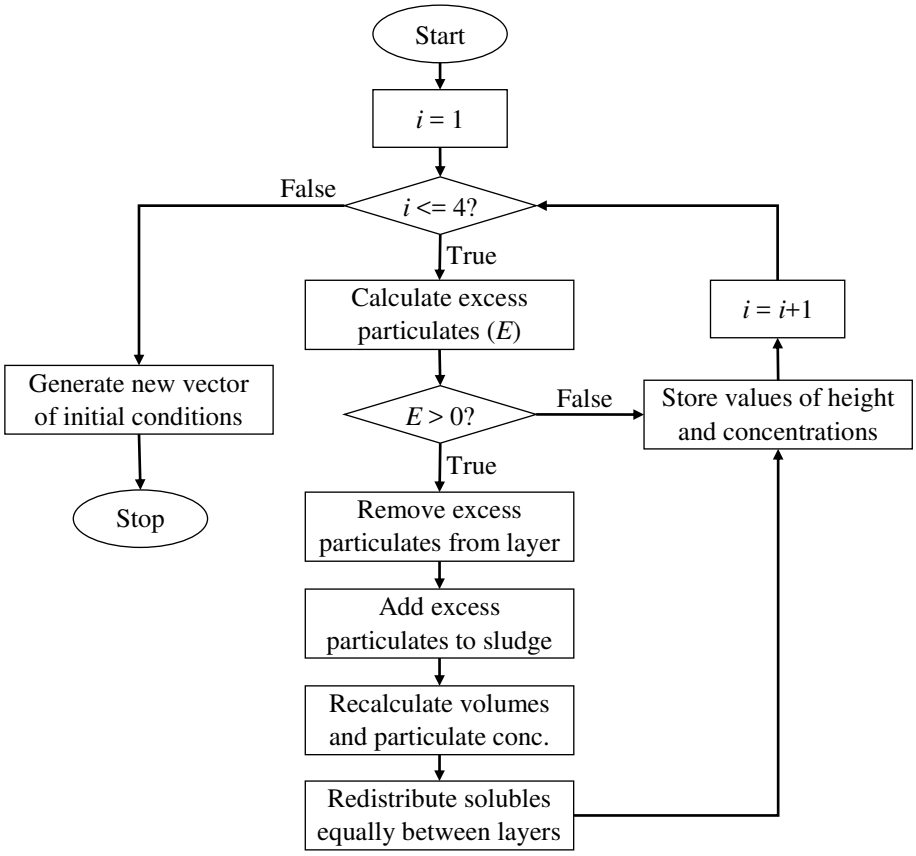

Figure B1. Flow chart describing the particulates and solubles redistribution between layers for the simulation of instant solids settlement (where $\boldsymbol{i = AE, AN, SL}$). Note: Excess particulates are transferred to the sludge layer without affecting the anaerobic liquid layer.

10. Flow rates distribution

Input wastewater is distributed between the aerobic, ice, anaerobic, and sludge layers by using the following conditions for selecting the flow rate between layers.

Condition	Time	Layer thickness	Input flow	Transfer flow
1. No icecap	$t \in \left[0, t_{ini}^{ICE}\right)$ or $t \in (t_{end}^{ICE}, 350]$	$z^{AN}(t) > 0$	$q_{in}^{AE*} = \left(\frac{1}{2} - \frac{\alpha}{2}\right) q_{in}$ $q_{in}^{AN*} = \left(\frac{1}{2} - \frac{\alpha}{2}\right) q_{in}$ $q_{in}^{S*} = \alpha q_{in}$ $q_{in}^{ICE} = 0$	$q_{tr}^{AE \to AN} = -q_{in}^{AE*}$ $q_{tr}^{AN \leftarrow AE} = q_{in}^{AE*}$
2. Icecap formation	$t \in \left[t_{ini}^{ICE},\ t_{ini}^{ICE} + \Delta t_{ini}^{ICE}\right)$	$z^{AN}(t) > 0$	$q_{in}^{AE} = 0$ $q_{in}^{AN} = q_{in}^{AN*}$ $q_{in}^{S} = q_{in}^{S*}$ $q_{in}^{ICE} = q_{in}^{AE*}$	$q_{tr}^{AN \to ICE} = q_{in}^{AE*} - \gamma_1$ $q_{tr}^{ICE \leftarrow AN} = -q_{in}^{AE*} + \gamma_1$
3. Icecap saturation	$t \in \left[t_{ini}^{ICE} + \Delta t_{ini}^{ICE},\ t_{end}^{ICE} - \Delta t^{ICE}\right)$	$z^{AN}(t) > 0$		$q_{tr}^{AN \to ICE} = q_{in}^{AE*}$ $q_{tr}^{ICE \leftarrow AN} = -q_{in}^{AE*}$
4. Icecap melt	$t \in (t_{end}^{ICE} - \Delta t_{end}^{ICE},\ t_{end}^{ICE}]$	$z^{AN}(t) > 0$		$q_{tr}^{AN \leftarrow ICE} = q_{in}^{AN*} + \gamma_2$ $q_{tr}^{ICE \leftarrow AN} = -q_{in}^{AN*} - \gamma_2$
4. Icecap limited	$t \in \left[t_{ini}^{ICE}, t_{end}^{ICE}\right]$	$z^{AN}(t) = 0$ $z^{ICE}(t) < z_{max}^{ICE}$	$q_{in}^{AE} = 0$ $q_{in}^{AN} = 0$ $q_{in}^{S} = q_{in}^{S*}$ $q_{in}^{ICE} = q_{in}^{AE*} + q_{in}^{AN*}$	None

where $\gamma_1 = \frac{A}{\Delta t_{ini}^{ICE}} \cdot (z_{max}^{ICE} - z_{max}^{AE})$ and $\gamma_2 = \frac{A}{\Delta t_{end}^{ICE}} \cdot (z^{ICE}(t_{end}^{ICE} - \Delta t^{ICE}) - z_{max}^{AE})$